



ELSEVIER

Contents lists available at [SciVerse ScienceDirect](http://SciVerse.ScienceDirect.com)

Optics & Laser Technology

journal homepage: www.elsevier.com/locate/optlastec

Scour monitoring system of subsea pipeline using distributed Brillouin optical sensors based on active thermometry

Xue-Feng Zhao^{a,*}, Le Li^a, Qin Ba^a, Jin-Ping Ou^{a,b}

^a School of Civil Engineering, Dalian University of Technology, Dalian 116024, PR China

^b School of Civil Engineering, Harbin Institute of Technology, Harbin 150090, PR China

ARTICLE INFO

Article history:

Received 6 January 2012

Received in revised form

28 February 2012

Accepted 12 March 2012

Keywords:

Subsea pipeline

Scour monitoring

Brillouin optical sensors

ABSTRACT

A scour monitoring system of subsea pipeline is proposed using distributed Brillouin optical sensors based on active thermometry. The system consists in a thermal cable running parallel to the pipeline, which acquires frequency shift of optical sensors during heating and cooling, directly indicating temperature change. The free spans can be detected through the different behaviors of heat transfer between in-water and in-sediment scenarios. Three features were extracted from temperature time histories including magnitude, spatial continuity and temporal stability. Several experimental tests were conducted using the proposed system. The results substantiate the monitoring technique.

© 2012 Elsevier Ltd. All rights reserved.

1. Introduction

The increasing world demand for and decreasing inland storage of oil and gas bring up a worldwide expansion of offshore hydrocarbon exploration. As the lifeline of subsea oil and gas transmission, subsea pipeline systems are widely used and greatly valued. Scour under subsea pipelines is a serious problem, perplexing engineers and researchers who try to maintain the pipeline systems throughout the service life. Typically, subsea pipelines are embedded into sea bed with depth of 1–1.5 m during installation process. However, the current around the pipes will gradually remove the cover and foundation of the pipes. That is the reason for hanging problem. Once the hanging length exceeds the design limit, local stress beyond ultimate stress in the pipes will lead to the structure failure. Furthermore, vortex-induced vibration can also lead to fatigue damage of the pipeline in a less hanging length. Therefore, the hanging length due to scour is a key parameter that determines the safety of pipes. According to Arnold's statistical analysis, scour and seabed movement were the major cause for subsea pipeline failure in Mississippi River delta from 1958 to 1965, which accounted for 36.2%, much higher than corrosion (29.2%) and machinery damaging (26.6%) [1]. According to Demars' analysis, corrosion, scour, third party activity and seabed movement were the four main causes of pipeline failure in the Gulf of Mexico during 1967–1975 [1]. A survey conducted on the 61 pipelines in Cheng

Dao oil field of China in 2004 showed that only five (8%) of them did not suffer hanging problem due to scour [2]. Therefore, scour under subsea pipelines needs to be timely monitored, reasonably evaluated and effectively controlled.

In recent years, optical fibers have been increasingly used in many fields for their peculiar advantages such as small size, high sensitivity, immunity to electromagnetic interference, low signal decay, accessibility to harsh environment, long-term measurement stability, etc. These advantages promise wide application of optical fibers in a subsea pipeline system, which is miles long and surrounded by complex and turbulent hydrodynamic and geographic environment. Due to the long distances to be monitored and the linear nature of pipelines, among the many optic sensing techniques, distributed fiber optic sensing techniques show significant advantages by providing distribution of the strain and temperature along the sensing optical fiber in both space and time domain. Fully distributed optical fiber sensors are based on Optical Time Domain Reflectometry technology. It uses a fiber, every bit of which acts as sensing element as well as data transmitting medium, to play the role otherwise played by numerous isolated sensors, reducing cost largely. To batter scour problem, many researchers attempted to use distributed optical fiber sensors to detect free spans of pipelines. Jin et al. successively proposed to detect free spans through natural vibration frequency of a pipeline (2003) [3] and an adapted Auto-Regression Model (2006) [4]. Elshafey et al. (2011) proposed strains variation on a pipe surface as an indicator of inception of free spans [5]. All of the methods mentioned above are based on distributed optical fiber sensors to monitor strain. While these attempts contribute to significant progress, they all focus on

* Corresponding author. Tel.: +86 411 8470 6443; fax: +86 411 84706414.

E-mail address: zhaoxuefeng1977@gmail.com (X.-F. Zhao).

indirectly measuring free span vibration or strain. There are two limits of research work mentioned above: First, for non-distributed strain sensors and accelerometers, only local information of pipelines can be monitored. Second, for distributed optical strain sensors, it is very difficult to install them along the pipelines.

In this paper, a scour monitoring system is presented based on active thermometry and distributed Brillouin optical fiber sensors. The distributed Brillouin optical sensors are used for sampling temperature, in order to monitor distributed scour status of subsea pipelines. Active thermometry is an effective way to measure thermal parameters [6,7]. Krishnaiah et al. measured thermal resistivity, thermal diffusivity and specific heat of rocks using thermal probe (2004) [8]. Keith L. demonstrated the capability of thermal probe by measuring thermal properties and volumetric water content of unsaturated sandy soil (1998) [9]. Freifeld et al. had developed a borehole methodology to estimate the ground surface temperature history by monitoring thermal conductivity profile along the length of a wellbore using fiber-optic distributed temperature sensor (2008) [10]. Sayde et al. demonstrated the feasibility of the active thermometry implemented with Raman fiber optical temperature sensors to obtain accurate distributed measurement of soil water content (2010) [11]. Cote developed a water leakage monitoring system of dam using distributed optical fiber temperature sensors (2007) [12]. The proposed monitoring system consists in an armored thermal cable running parallel to the subsea pipelines, which consists of three main components: a heating belt, optical fibers, and packing elements. The heating belt radically releases heat and the fibers concurrently measure temperature. The surrounding environment, sediment or water, can be identified by analyzing the acquired data of frequency shift, thus estimating the interface position and the free span length. The armored cable can be installed along the pipes in the vicinity, and does not need to be mounted on the surface of the pipes. This means that when sour happens, the pipes and the cable will be exposed to water at the same time and same location. Because during the pipelines construction, the pipes are welded together on boats, and then putted into the sea bed, it is almost impossible to install the distributed fiber optical strain sensors along the pipes. Scour monitoring system proposed in this paper can make the installation of distributed fiber optical temperature sensors along pipes possible. The mechanism of scour monitoring breaks the above two limitations. This flexibility saves many construction problems and makes it highly applicable to practice.

2. Theory background

2.1. Principle of Brillouin optical fiber sensing technique

Brillouin scattered light starts up in the interaction between the laser light in the optical fiber with the acoustic phonons. And there will be a Brillouin gain (BG) if there exists a reverse propagating light in the Brillouin gain frequency band. Brillouin frequency shift changes in proportion to the temperature of the fiber and the strain applied to the fiber. The relationship is expressed as [13]:

$$\begin{cases} \nu_B(\varepsilon) = \nu_b(0) + C_\varepsilon \varepsilon \\ \nu_B(T) = \nu_b(T_0) + C_t(T - T_0) \end{cases} \quad (1)$$

where $\nu_B(\varepsilon), \nu_b(0), \nu_B(T), \nu_b(T_0)$ are frequency shifts under strain ε and 0, and under temperature T and T_0 , respectively. C_ε and C_t are strain coefficient and temperature coefficient, respectively. Assuming no strain exists, thus

$$\Delta \nu_B = C_t \Delta T \quad (2)$$

where $\Delta \nu_B = \nu_B(T) - \nu_B(T_0)$ is defined as frequency shift and $\Delta T = T - T_0$ is defined as excess temperature.

2.2. Heat transfer behaviors in solid and liquid

Modes of heat transfer in liquid and in water are convection and conduction, respectively. For heat conduction in solids, our problem can be idealized as an infinite line source in an infinite, homogeneous, isotropic medium. By using "Transient heat method" [14], for large value of t ($t \gg r^2/(4\alpha)$) and $t - t_1 \gg r^2/(4\alpha)$, respectively),

$$\begin{cases} \Delta T = \frac{q}{4\pi\lambda} \left(\ln t + \ln \frac{4\alpha}{r^2} - \gamma \right) & t \leq t_1 \\ \Delta T = \frac{q}{4\pi\lambda} \ln \frac{t}{t - t_1} & t > t_1 \end{cases} \quad (3)$$

where ΔT is the excess temperature; $\Delta T = T - T_0$; T_0 is initial temperature; γ the Euler's constant ($\gamma = 0.5772$); q the quantity of heat released per unit length of the line source during heating, which starts at $t = 0$ and stops at $t = t_1$; α the thermal diffusivity of the solid ($\alpha = \lambda/\rho c$); λ , ρ , c are the thermal conductivity, the density and the specific heat of the solid, respectively. r the distance to line source. t_1 the time heat stops.

For heat convection in a liquid, in this study, the thermal resistance of the thermal cable can be neglected due to the small cross-section area of the thermal cable. The lumped parameter method is adopted by assuming the inner temperature is uniform within any given cross section of the thermal cable. The problem is simplified to

$$\begin{cases} \rho c V \frac{\partial T}{\partial t} = q - Ah(T - T_0); & t \leq t_1 \\ \rho c V \frac{\partial T}{\partial t} = -Ah(T - T_0); & t > t_1 \\ T = T_0; & t = 0 \end{cases} \quad (4)$$

where h is the convective heat transfer coefficient; ρ and c are the density and the specific heat, and A and V are the convective area and volume per unit length of the sensor, respectively. The solution is

$$\begin{cases} \Delta T = \frac{q}{hA} (1 - \exp(-t/\tau_c)) & t \leq t_1 \\ \Delta T = (T(t_1) - T_0) \cdot \exp(-t - t_1/\tau_c) & t > t_1 \end{cases} \quad (5)$$

with $\tau_c = \rho c V / hA$, which is called time constant.

3. Material and methods

3.1. Scour monitoring system setup

The scour monitoring system was comprised of a thermal cable with an external power supply, Data Acquisition Unit (DAU) and Data Processing Unit (DPU), as showed in Fig. 1. The thermal cable consisted of a heating belt, armored optical fibers and hot pyrocondensation pipes. The self-regulating heating belt was 21 m long and of a cross section dimensions of 2 mm × 10 mm, whose maximum power and maximum surface temperature were 25 w/m and 80 °C, respectively. The armored optical fibers were glued on the heating belt using 502 glue. To be protected from water, they were carefully capsulated in hot pyrocondensation pipes of 16 mm diameter. The measurement was based on BOTDA (Brillouin Optical Time-Domain Analysis). The optical fibers were connected to an analyzer, forming a loop. The analyzer, DiTes tTM STA100/200 Series-Fiber Optic Distributed Temperature and Strain Analyzer, acted as the DAU. Configuration of the analyzer is showed in Table 1. The optical fiber sensors sampled frequency shift every six minutes. The data were transmitted to a laptop to be stored and analyzed, which acted as the DPU. Maximum length of one single strand of heating belt was 100 m. For distributed scour monitoring of subsea pipelines over long distance, parallel

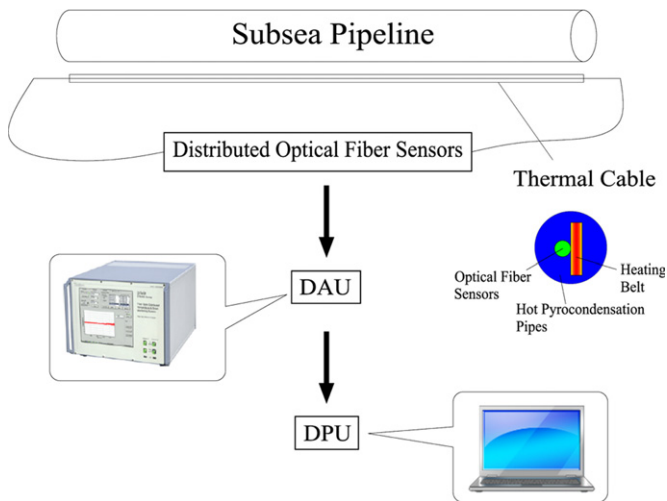


Fig. 1. System overview.

Table 1
Configuration of analyzer.

Spatial resolution	1.0 m
Sampling interval	0.41 m
Central frequency	10.9255 GHz
Frequency step	0.003 GHz
Sampling time interval	6 min



Fig. 2. Experiment setup.

circuit can be utilized to build long linear heater by connecting the 100 m long heating belts together. There is a problem of relative large energy consumption due to the big electrical power needed over long sensing distance. However, comparing with the cost of traditional distributed pipeline scour investigation aided by Remote Operated Vehicle (ROV), divers and sonar boats, it is acceptable. Especially, the scour monitoring system will not be affected by subsea and weather condition with high monitoring frequency.

3.2. Scour monitoring system experiments

Tests were conducted in the laboratory of hydraulic engineering at Dalian University of Technology to validate the monitoring technique. A 21 m long section was partitioned from a 48 m long water channel with both ends blocked by brick walls. The water

channel was 1 m wide and 1.5 m high with a water inlet and outlet in each end. The brick walls were 0.6 m high and could let water pass through. A controllable water cycle was created by using a pump at the outlet of the water channel so that the experiments were conducted in a running water environment. Three 6 m long steel tubes were welded end-to-end to form an 18 m long steel tube. Each tube had a diameter of 100 mm and a thickness of 2.5 mm. Ends and joints of the welded tube were waterproofed. The tube was subsequently placed in the middle of the separated water channel section, with a distance of 20 cm to the bottom, acting as a subsea pipeline (Fig. 2). The thermal cable ran parallel to the tube with each end of the cable extending 1.5 m past the end of the tube (Fig. 2). The cable was secured to the tube using custom-made hooks with a length of 5 cm and 1 m spacing. To create a scenario with free span of subsea pipeline, the 21 m water channel was partitioned into three sections by using brick walls that allowed water to pass. The two outer sections were roughly 7 m long and filled with sand; the sand was 50 cm high and served as sediment. The middle section was 6 m long and devoid of sand; it was used to simulate the free span (Fig. 2).

To fully saturate the sand before the experiments were performed, water was continuously added into the water channel to maintain a constant water level of 70 cm for 2 h. Then three tests were conducted as follows: First, turn on the analyzer and computer; the optical fibers start sampling, lasting for 5 min. Then connect the heating belt to the power; it starts to generate heat. Lastly, after heating for some time, disconnect the heating belt, it begins to cool down, keep sampling for some time before turn off the analyzer. The first test consisted of 2 h of heating and 1 h of cooling. Both the second and the third test consisted of 3 h of heating and 1 h of cooling. The room temperature was recorded every 30 min throughout the test.

4. Results and discussion

Raw data of frequency shift in the first test show notable abnormality during the distance around 22–27 m (Fig. 3). As indicated in Eq. (2), after frequency shift subtracting the corresponding values acquired before heating and multiplied by temperature coefficient, excess temperature during heating and cooling is obtained (Fig. 4). The temperature coefficient is attained through several calibration tests in advance, which is 1.027 °C/MHz in this study.

Each curve in Fig. 4 represents the sampling data of one scanning. Label the section 21.57–26.86 m M and the neighborhood sections L and R. Section M clearly distinguishes itself,

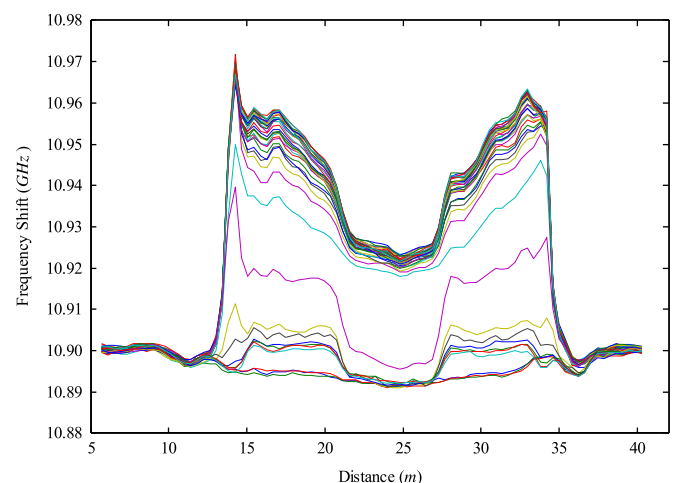


Fig. 3. Frequency shift along the optical fibers for test 1.

which can be identified through three features extracted from the curves of excess temperature. The first feature is magnitude. The curves within M are lower than those within R and L. By calculating the average excess temperature of all the sampling points during heating period, a notable temperature gap around 20 °C is quantified between the identified section M and section L or R (Fig. 5 and Table 2). The second feature is temporal stability. The excess temperature curves within section M are more stable along time, which mainly fall into two comparatively concentrated branches, while curves within sections L and R are distributed along the vertical axis. The third feature is spatial continuity. The excess temperature curves within M show good continuity over locations, which are almost parallel to the horizontal axis, while curves within section L and R tend to sway up or down. The latter two features can be quantified by variance

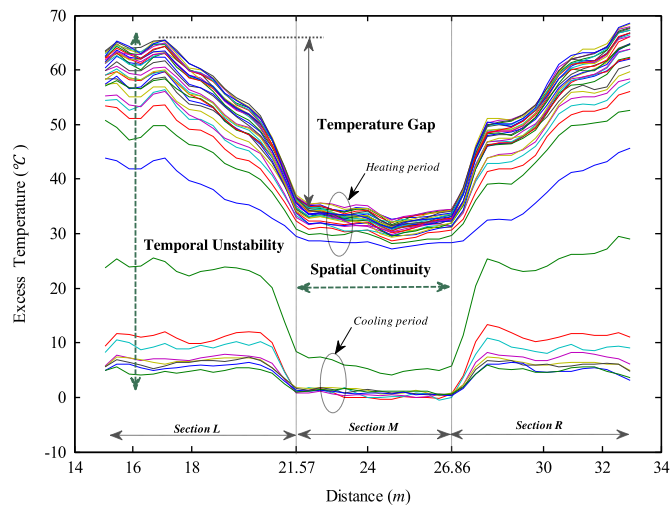


Fig. 4. Excess temperature in the range of heating belt for test 1.

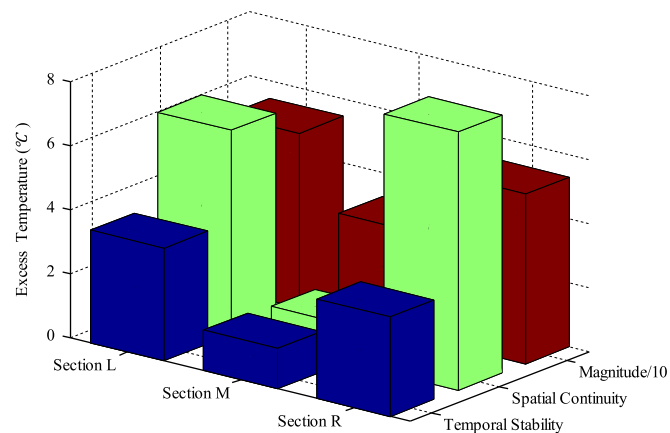


Fig. 5. Three features of excess temperature curves for test 1.

Table 2
Three features of excess temperature curves for the three tests (°C).

Section	Test 1			Test 2			Test 3		
	L	M	R	L	M	R	L	M	R
Magnitude	54.60	32.60	53.12	52.35	33.87	52.36	52.63	34.16	53.02
Spatial continuity	6.381	1.182	8.072	4.271	1.375	5.674	3.081	1.473	5.627
Temporal stability	3.519	1.260	3.113	4.412	1.062	4.288	3.523	1.089	3.457

with time and location, respectively (Fig. 5 and Table 2). Likewise, these three features can be calculated for the other two tests (Fig. 6 and Table 2). These results show considerable distinction between in-water and in-sediment scenarios, making the detection of free span possible.

The three features are the results of the different mechanisms of heat transfer between in-sand and in-water scenarios. Generally, heat dissipates more easily through convection via water than conduction via sand. While it dissipates gradually through conduction in sand, heat can be directly carried away by flow. Excess temperature in sand and in water has a logarithmic and exponential relationship with time, respectively (Eqs. (3)–(5)). In sand, it climbs according to formulas $(\ln t + \ln 4\alpha/r^2 - \gamma) \cdot q / (4\pi\lambda)$ and $\ln(t/t - t_1) \cdot q / (4\pi\lambda)$ (Eq. (3)) during heating and cooling period. In water, it exponentially rises up to a plateau (q/hA) when heat starts, and exponentially drops down back to a flat (zero) when heat stops (Eq. (5)). This directly leads to the first two features. First, for most of the possible thermal parameters in subsea environment, $(\ln t + \ln 4\alpha/r^2 - \gamma) \cdot q / (4\pi\lambda)$ will be larger than q/hA in several seconds, plus $\ln t/t - t_1 \cdot q / (4\pi\lambda)$ is larger than zero. Therefore, average excess temperature is higher in sediment than in water. And a greater flow rate leading to a greater h will enlarge the temperature gap. Second, in water temperature changes so fast that the increasing and decreasing processes can be hardly captured by sampling with a relatively large time interval 6 min. So excess temperature falls into curves of two branches, corresponding to the plateau during heating period and flat during cooling period, respectively. While in sand, temperature changes more slowly and lastingly, making the changing process traceable. So the excess temperature curves spread out. Furthermore, swiftness of heat transfer in water makes the temperature more uniform across different locations. Contrarily, locations in sand are comparatively more isolated without much interplay. So temperature in sand presents larger variability between different locations. Overall, these three features of temperature curves are justifiable to identify the free span.

To obtain the free span length, the length of M (26.86–21.57=5.29 m) should be added by the resolution length of the optical fiber (1 m). According to Brillouin optical fiber sensing technique, the signal of a sampling point on the optical fiber is not the signal of the specific sampling point, but the average signal within a certain range relating to that point. This range is the spatial resolution. Consequently when the section M is identified meeting the features of temperature change of in-water scenario, it does not mean M is the entire free span section, but indicates that the locations within the resolution ranges of all the sampling points that yield the data of section M are all immersed in water. So the identified free span is 6.29 m long, which is 0.29 m different from the experimental setup. Theoretically, the resolution of the monitoring system is twice the sampling interval of the optical fiber, which is 0.82 m in this case, with both sides a possible maximal error of a sampling interval to the interface. Considering the actual pipeline is miles long, this level of precision is satisfying.

However, near the water-sand interfaces, sand and water interplay in heat transfer. It is a fluid-solid coupling problem. The analytic solutions Eqs. (3) and (4) are not applicable. It leads

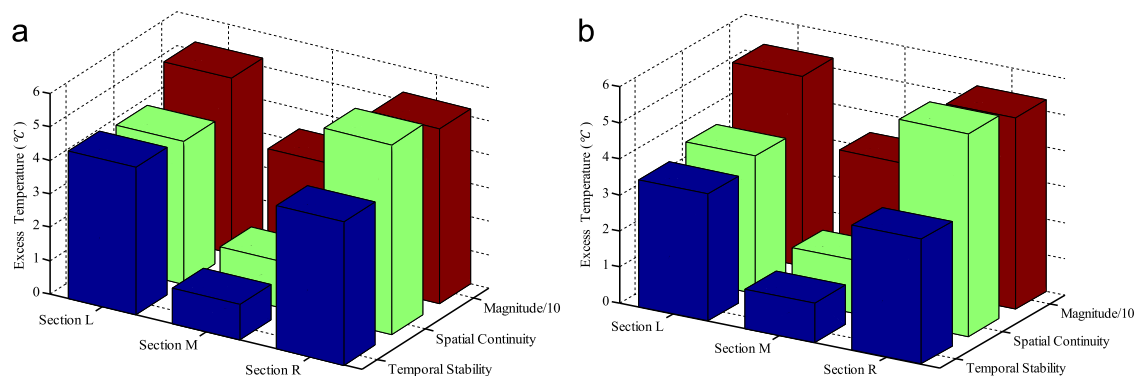


Fig. 6. Three features of excess temperature curves; (a) for test 2. (b) for test 3.

to transition parts of temperature distribution on both ends of the free span and, to some extent, blurs the distinction between in-sediment and in-water scenarios. The existing of transition parts adds difficulties and, probably, errors to the identification of section M and therefore, adversely affects the precision. Though the experimental results seemly showed no need for fuss about the effect of the transition parts, accurately evaluating to what extent the effect is calls for further research, which requires endeavors of prudent simulation, field experiments and detailed researches on the practical environment where the pipelines stands.

Finally, in contrast to the current monitoring strategy [3–5], the proposed system is based on active thermometry, which relies on its own, known, heat source rather than on an external natural source. It renders high reliability. More importantly, the monitoring technique focuses right on the scour consequence rather than the free span vibration. There is no need for the thermal cable to be packaged inside pipelines. It can work just deployed in the vicinity of pipelines, which makes construction of the system flexible and therefore suitable for practical application.

5. Conclusions

A scour monitoring system of subsea pipeline is proposed. The system is based on active thermometry and distributed Brillouin optic sensing techniques. Experimental tests demonstrated the feasibility of the monitoring system. The free spans can be quickly detected through three features extracted from the acquired data of frequency shift, including small magnitude of excess temperature; high stability along time; and low discreteness over location. The system presented promising application future for its high reliability, low cost, high precision and construction flexibility.

Acknowledgments

Thanks for the financial supports of National Basic Research Program of China (2011CB013702), Key Projects in the National

Science & Technology Pillar Program during the Twelfth Five-Year Plan Period (2011BAK02B02) and National Natural Science Foundation of China (5092100).

References

- [1] HERBICH JB. Offshore Pipeline Design Elements. New York: Marcel Dekker Inc.; 1981.
- [2] Meng F, Xu A, Li J. Control of hanging problem of offshore subsea pipeline. China Offshore Platform 2006;1:52–4.
- [3] Jin W, Shao J, Zhang E. Basic strategy of health monitoring on submarine pipeline by distributed optical fiber sensor. ASME Conference Proceedings 2003;36827:531–6.
- [4] Jin W, Shao J. A practical algorithms on health monitoring of submarine pipeline and its application. ASME Conference Proceedings 2006;47497:309–13.
- [5] Elshafey AA, Haddara MR, Marzouk H. Free spans monitoring of subsea pipelines. Ocean Systems Engineering 2011;1:59–72.
- [6] Campbell GS, Calissendorff C, Williams JH. Probe for measuring soil specific heat using a heat-pulse method. Soil Science Society of America Journal 1991;1:291–3.
- [7] Bristow KL, Campbell GS, Calissendorff K. Test of a heat-pulse probe for measuring changes in soil water content. Soil Science Society of America Journal 1993;4:930–4.
- [8] Krishnaiah S, Singh DN, Jadhav GN. A methodology for determining thermal properties of rocks. International Journal of Rock Mechanics and Mining 2004;5:877–82.
- [9] Bristow KL. Measurement of thermal properties and water content of unsaturated sandy soil using dual-probe heat-pulse probes. Agricultural Forest Meteorology 1998;2:75–84.
- [10] Freifeld BM, Finsterle S, Onstott TC, Toole P, Pratt LM. Ground surface temperature reconstructions: using in situ estimates for thermal conductivity acquired with a fiber-optic distributed thermal perturbation sensor. Geophysical Research Letters 2008;L14309.
- [11] Sayde C, Gregory C, Gil-Rodriguez M, Tuffillaro N, Tyler S, van de Giesen N, et al. Feasibility of soil moisture monitoring with heated fiber optics. Water Resources Research 2010;W6201.
- [12] Cote A, Carrier B, Leduc J, Noel P, Beauchemin R, Soares M, et al. Water leakage detection using optical fiber at the Peribonka dam. ASCE Conference Proceedings 2007.
- [13] G.Y.D. Guideline for the design of a fiber optic distributed temperature and strain sensor. Optical Communications 2007;1:227–37.
- [14] de Vries DA, Peck AJ. On the cylindrical probe method of measuring thermal conductivity with special reference to soils. I extension of theory and discussion of probe characteristics. Australian Journal of Physics 1958;2:255–71.